

# Spatiotemporal laser perturbation of competing ionization waves in a neon glow discharge

K.-D. Weltmann,\* M. E. Koepke, and C. A. Selcher†

*Department of Physics, West Virginia University, Morgantown, West Virginia 26506-6315*

(Received 28 July 1999; revised manuscript received 15 May 2000)

The experimental verification of spatiotemporal periodic pulling, a specific but universal phenomenon associated with driven, nonlinear, spatiotemporal systems, is reported as part of a study characterizing the ability of dc and chopped laser light to induce periodic pulling in ionization waves propagating in a neon glow-discharge plasma. The degree to which a single-mode laser beam at a metastable transition of  $6401 \text{ \AA}$  ( $1s^5-2p^9$ ) influences the discharge is found to depend on the location and magnitude of the perturbation. Cases of ac (chopping the light) and dc perturbation are presented. In a range of chopping frequencies above and below the ionization wave's undriven frequency, the wave can become synchronized to the perturbation. This entrainment range is shown to depend on the frequency difference between the wave and the perturbation, as well as on the perturbation distance from the cathode. Hysteresis is found in the value of the perturbation frequency associated with transitions into and out of entrainment. Outside of entrainment, periodic pulling of a self-excited, propagating, ionization wave by the laser perturbation is observed. This is a case of frequency pulling, or temporal periodic pulling. Inside of entrainment, the chopped laser light controls the frequency and amplitude of the mode. By properly adjusting the frequency and amplitude of one mode with respect to a second mode, periodic pulling of one ionization wave by the mode-locked, propagating, original ionization wave is demonstrated. This is a case of spatiotemporal pulling, involving both wavelength pulling and frequency pulling. Under proper conditions, competition between temporal and spatiotemporal periodic pulling results in a modulation in the dynamics of the system, a process referred to as dynamics modulation.

PACS number(s): 52.35.-g

## I. INTRODUCTION

The dynamic behavior of a glow discharge is determined by all regions of the discharge, such as the Aston dark space, cathode dark space, cathode layers, Faraday dark space, positive column, anode dark space, and anode glow [1]. The neon glow discharge can be operated as a multimode oscillator since the positive column can support waves, manifest as individual oscillatory modes, that propagate along the tube. These waves, also referred to as moving striations, can be excited spontaneously or by an externally applied perturbation, depending on the system's important parameters, such as pressure, boundaries, discharge voltage, and discharge current [2,3]. For a given set of ambient parameter values, a particular oscillatory mode dominates. By incrementing the ambient parameter values, modes that differ by the integer number of axial wavelengths can be excited in sequence. For certain parameters, two different modes, one dominant and the other subdominant, may coexist, each with a specific frequency and wavelength determined by the plasma conditions near the cathode. These plasma conditions are strongly influenced by the gas pressure, tube boundaries, and external circuit, which are kept fixed here, as well as the discharge current, which is adjusted to different values in these experiments.

The effect of the waves at the anode feeds back to the cathode via the external circuit and is responsible for processes involved in the natural selection of one dominant mode [2,4]. The amplitude of a wave excited by a periodically varying perturbation of one of the important control parameters is found to maximize at a perturbation frequency approximately equal to one of the spontaneously excitable mode frequencies, with submaxima when the frequency of the perturbation, or driving force, is a harmonic or subharmonic of the mode frequency [5,6].

The relative mode amplitude is determined by mode competition and exhibits hysteresis as the discharge current is incremented upward and downward [2,7,8] (cf. Fig. 3). As the discharge current is incremented and a mode transition is induced, it becomes energetically favorable for the original subdominant mode to become dominant. During the instant that the dominant mode switches from one frequency to the other, the growing subdominant mode is large enough to strongly interact with the original dominant mode. Without additional control of the individual mode frequency and amplitude, the deviation of mode frequency from its ambient value during this transition, although reproducible, is uncontrollable, limited in extent ( $\Delta f/f < 25\%$ ), and very brief ( $\Delta t < 20 \text{ ms}$ ). Laser light can induce mode transitions as well, but it also can provide mode-frequency control for mode-transition investigations when the beam is periodically chopped at frequencies comparable to the mode's undriven frequency. The nonlinear interaction known as periodic pulling [9–11], which occurs during mode transitions [8], is investigated using the advantages of chopped-laser-beam control of the interaction. In this paper, we perform a systematic characterization of the ability of dc and chopped laser light

\*Permanent address: ABB Corporate Research Ltd., CH-5405, Baden-Dättwil, Switzerland.

†Now at Code 5551, Naval Research Laboratory, Washington, DC 20375.

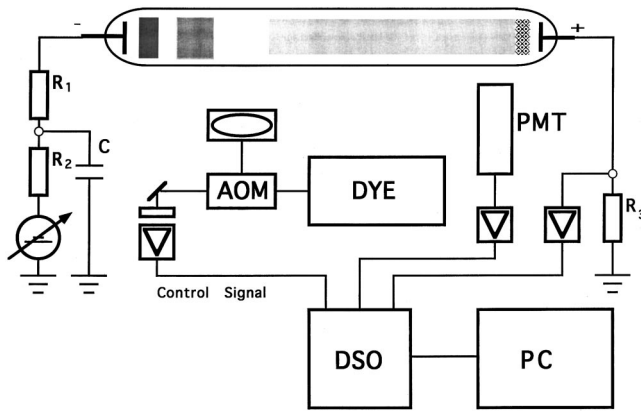


FIG. 1. Experimental arrangement.

to induce periodic pulling in ionization waves. A preliminary report was presented earlier [12].

## II. EXPERIMENTAL APPROACH

Investigations were carried out using a conventional glass discharge tube [7,13] (length  $L = 750$  mm, inner diameter 22 mm) with a hollow cathode and a plane anode, filled with neon gas at pressure  $P = 170$  Pa. Figure 1 is a diagram of the experimental configuration. Tube-radius/pressure/discharge-current parameter space can be divided into striation-free (homogeneous) and spontaneous-striation regions. The latter region can be further divided into specific classes of spontaneous striations [14]. The self-excited ionization waves investigated here are the  $p$  striations.

The discharge is operated with load resistor  $R_L = 100$  k $\Omega$  at a discharge current  $I_D = 2$ –20 mA. To study driven-oscillator behavior, the discharge can be externally modulated at a frequency  $f_D$  by an ac-coupled, sinusoidal component of the discharge voltage [7,8,15–17]; however, in this paper, we instead use the chopped, neon-resonant light beam from a tunable, narrowband dye laser as the external driving force. The 2-mm-diam laser beam (center wavelength of 6401 Å, 4 nm filter) can be positioned anywhere along the tube. The ionization waves are measured by means of light flux fluctuations  $\Phi(t)$ , the time series of which are recorded with digitizers. The *instantaneous frequency*, used to temporally resolve the frequency modulation in the system response, is determined from the time series by inverting the period between pairs of zero crossings spaced an oscillation period apart [11].

Light flux from the discharge, which indicates some important properties of the glow discharge, has been used to determine information related to elementary processes such as collision rates [18]. Important to our experiments is the variation in the light flux with position along the tube even when no striations are present. Figure 2 shows axial profiles of the time-integrated intensity from the most intense neon emission line and absorption line (6401 Å) for three values of discharge current for homogeneous conditions in the  $p$ -striation regime. For this plot, mode transitions are suppressed by using a current source instead of the voltage source to sustain the discharge [16]. Apparent in each profile is an increase of the light from approximately zero intensity, in the cathode region ( $0 < z < 5$  cm), to a large intensity

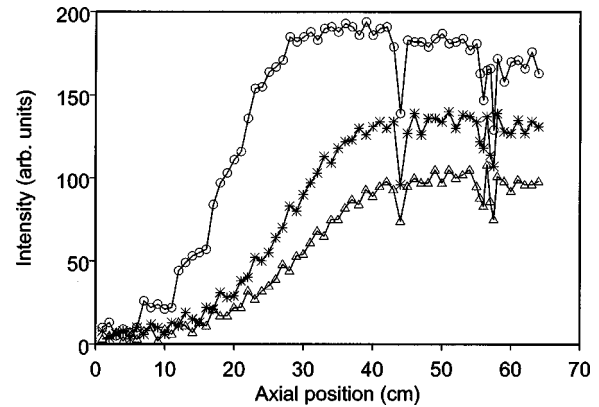


FIG. 2. Intensity of neon line (center wavelength of 6401 Å, 20 nm filter) emission along plasma column. No laser perturbation is applied. The discharge current is 4.47 mA (triangles), 5.47 mA (stars), and 7.47 mA (circles).

which is approximately uniform along the plasma column in the saturation region. The level and length of this region is different for each profile. An amplification region connects the cathode and saturation regions. Dips in the profile, about 20% deep and 2 mm in axial extent, correspond to the locations of three thin (10- $\mu$ m diameter), electrically floating, tungsten wires (Langmuir probes) inserted radially into the plasma to the cylindrical axis and are considered insignificant to the results presented in this paper.

## III. DISCRETE OSCILLATORY MODES OF THE IONIZATION WAVES

Each mode corresponds to a well-defined number of uniform striation wavelengths in the system [8]. At a given value of  $I_D$ , one mode dominates over all the others. As  $I_D$  is incremented toward the transition from one dominant mode to another adjacent in frequency, the prospective dominant mode becomes apparent as a low-amplitude secondary mode that competes for the available free energy of the system. The transition occurs abruptly at a precisely reproducible value of  $I_D$ , after which there are new values of striation frequency and discharge current, as well as an absence of secondary modes.

For values of  $I_D$  far from those associated with mode transitions, the discharge current, for a fixed value of discharge voltage, remains constant over a time period much longer than it takes to perform a typical sequence of experiments. Also, within this range, adjustments in the discharge current can be made by proportional adjustments in the discharge voltage. However, as the value of discharge voltage is smoothly ramped to span the operational range of the discharge current, sudden jumps occur in the discharge current at the mode transitions and, consequently, the ramp in the discharge current is not as smooth as that in the discharge voltage. Figure 3 shows the various modes, each with a distinct and narrow frequency range, that occur over a wide range of discharge current. The specific mode identified with a particular discharge current depends on the history of the discharge [1,2,14]. At the terminating point of each step in the stairlike plot in Fig. 3, a transition takes place to the next-higher frequency or next-lower frequency mode that

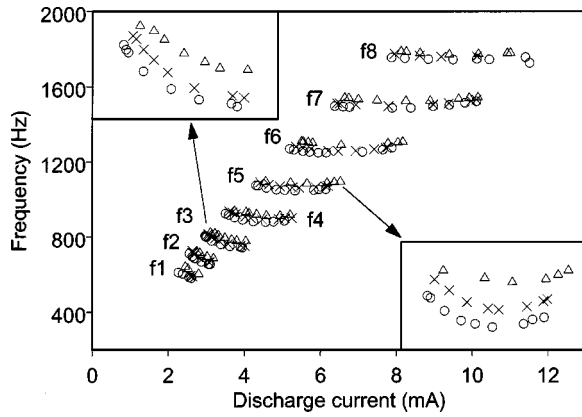


FIG. 3. Oscillatory modes of the neon glow discharge. The mode associated with a specific value of discharge current depends on the operating history of the device because of hysteresis. The effect of neon-resonant laser light is indicated: 0% intensity (circles), 50% intensity (stars), and 100% intensity (triangles). Data for two modes are expanded to better resolve this effect. Each mode is labeled by its undriven frequency in ascending order.

overlaps at that discharge current. The influence of the dc resonant laser light on the ranges of frequency and current associated with each mode is seen in Fig. 3 to be more noticeable for some modes than others. The inserts in Fig. 3 show an expanded view of this influence for two modes.

#### IV. MODE TRANSITIONS ACCOMPANIED BY A WAVE-WAVE INTERACTION

During the transition, the ratio of wave amplitudes rapidly passes from one extreme, through unity, to the other extreme. Correspondingly, the wave-wave interaction changes from weak, to strong, and back to weak. The signatures of

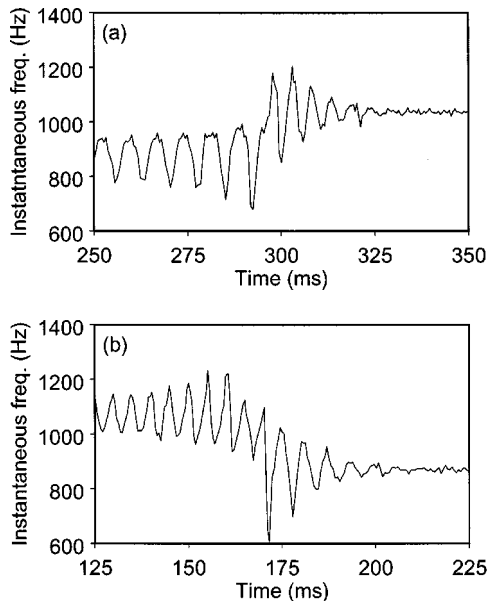


FIG. 4. Upward and downward transitions between two modes as the discharge current is incremented upward and downward, respectively. Time series and instantaneous frequency for transitions (a) from mode No. 4 to mode No. 5 and (b) from mode No. 5 to mode No. 4.

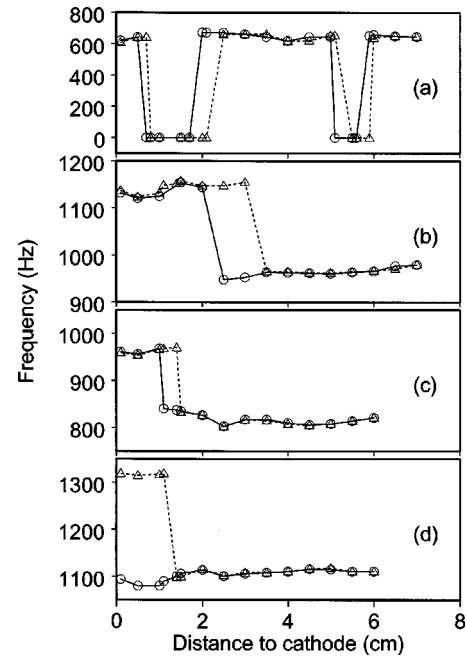


FIG. 5. Mode transitions between pairs of modes as the position of the dc laser perturbation along the plasma column is incremented back and forth. The triangles and circles correspond to moving away from and toward the cathode, respectively. The discharge current is (a) 2.51 mA, (b) 3.96 mA, (c) 3.98 mA, and (d) 5.52 mA.

spatiotemporal periodic pulling [8] are readily, but transiently, observed when the wave-wave interaction is strong. Figure 4 shows the time series and instantaneous frequency associated with the transition from the 1.5 kHz mode to the 1.75 kHz mode. Notice that the amplitude modulation and frequency modulation are synchronized and approximately sinusoidal and that the modulation depth is largest at the transition point. As reported by Koepke *et al.* [8,19], it is the growing secondary wave that drives the original dominant mode.

A transition between modes also can be induced by using laser light to perturb the positive column, as indicated in Fig. 3 by the sensitivity of the mode frequency to resonant laser light. However, the strength of the perturbation, at the chosen metastable transition, depends on the laser beam's axial location along the tube. Figure 5 shows various mode transitions as the distance between the laser beam and the cathode is first increased and then decreased in the vicinity of a transition point. Hysteresis in the location of the mode transition is apparent. The transitions in Fig. 5(a) are between the lowest-frequency mode and the striation-free regime. The transitions in Figs. 5(b)–5(d) are between two modes adjacent in frequency. In Figs. 6 and 7, the amplitude modulation and frequency modulation are documented for these cases and evidence of wave-wave periodic pulling is apparent. Notice that transitions induced by changing the laser beam position are similar to those induced by changing the discharge current.

#### V. CHOPPED, NEON-RESONANT, LASER LIGHT PROVIDES PERIODIC FORCING

By chopping the laser beam, a temporal, spatially localized perturbation drives the self-oscillating system. The

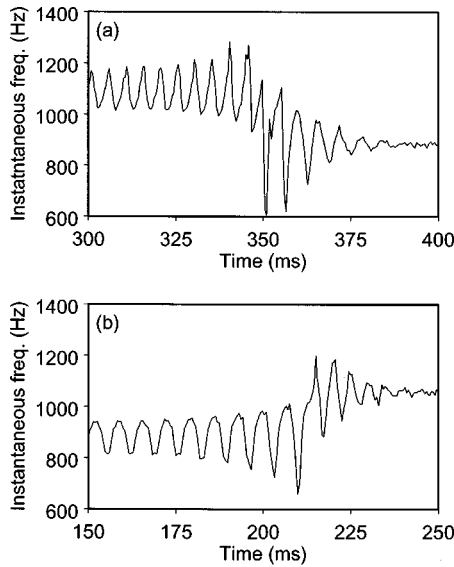


FIG. 6. Mode transitions between pairs of modes as the position of the dc laser perturbation along the plasma column is incremented back and forth. The discharge current is 4.5 mA. The distance from the cathode and direction of movement associated with each plot are (a) 2.75 cm, increasing and (b) 2.60 cm, decreasing.

chopping frequency is the driving frequency of this laser-wave perturbation and the light intensity and the extent to which the light is resonant with metastable transitions in neon are related to the driving amplitude. For a sufficiently large driving amplitude, the system is synchronous with the driving force within a limited driving-frequency range on either side of the self-oscillation, or undriven, mode frequency. This range in  $f_D$  depends on light intensity, but also on discharge current and the separation of the laser beam and the cathode, as shown in Fig. 8. The general size of the irregular shaped entrainment region in Fig. 8 maximizes at a

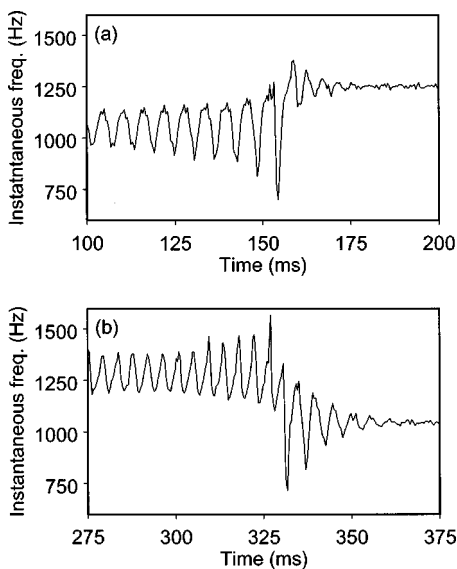


FIG. 7. Mode transitions between pairs of modes as the position of the dc laser perturbation along the plasma column is incremented back and forth. The discharge current is 5.2 mA. The distance from the cathode and direction of movement associated with each plot are (a) 3.10 cm, increasing, and (b) 2.95 cm, decreasing.

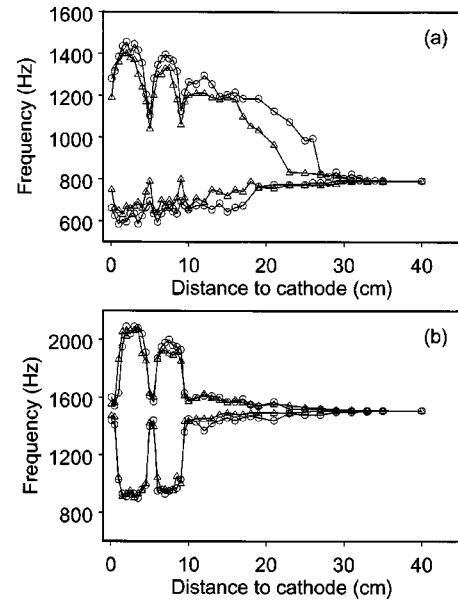


FIG. 8. Upper and lower entrainment boundaries in frequency as a function of position along the plasma column. The boundaries are obtained by first setting  $f_D = f_0$  and then carefully shifting  $f_D$  toward and across the upper or lower boundary. The discharge current is (a) 4.5 mA and (b) 7.5 mA. The laser intensity is 100% for the circles and 50% for the triangles.

different discharge current for each mode. Within this range, the oscillation amplitude of the system response is maximum for  $f_D \approx f_0$  and falls off to a minimum for driving frequencies at the limits of the entrainment range. The entrainment boundaries shown in Fig. 8 are obtained by first setting  $f_D = f_0$  and then carefully shifting  $f_D$  toward and across the upper or lower boundary. Entrainment boundaries associated with approaching  $f_0$  from *outside* the entrainment range are substantially closer together.

When the driving frequency is outside of the entrainment range, the temporal laser perturbation can periodically pull the system. When the driving frequency is within the entrainment range, the laser can be used to control the frequency, and thereby the wavelength, of the mode. When the entrained mode frequency and wavelength are shifted sufficiently close to those of the next-higher or next-lower mode, the two modes can interact via spatiotemporal, or wave-wave, periodic pulling. In this situation, two nonlinear interactions, the entrainment of one mode by the chopped laser light and the periodic pulling of one mode by the spatiotemporal perturbation of the other mode, are taking place simultaneously. The periodic pulling interaction is similar to the transient interaction described in the undriven cases of Figs. 4–7, except that this one is not transient. Instead, the laser driving force stabilizes the mode competition by maintaining the frequency separation between the perturbation and the mode and essentially sustaining the system partway between two of the stable limit cycles associated with the modes of the undriven system.

For example, spatiotemporal periodic pulling can be controlled by entraining a subdominant mode near its spontaneous frequency with chopped laser light, but two points deserve emphasizing. First, the chopped light significantly enhances the amplitude of (i.e., excites) the subdominant

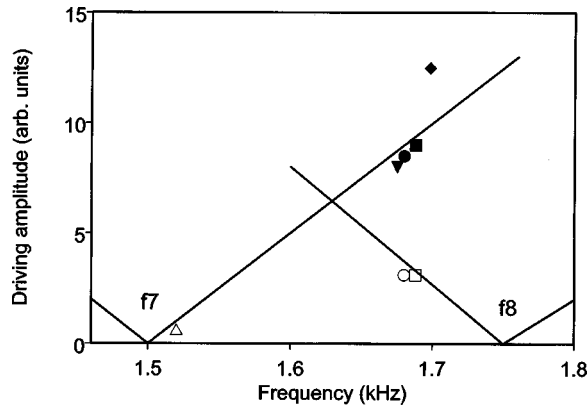


FIG. 9. Dynamics phase diagram for a multimode oscillator. The normalized vertical scale is in arbitrary units of  $M$ . The horizontal scale and the specific points are relevant to the neon glow discharge experiments reported here. The region above the v-shaped boundaries corresponds to entrainment for the mode identified by its undriven frequency, labeled (based on Fig. 3, using a subscript) where the v-shape contacts the horizontal axis. The open triangle, filled inverted-triangle, open and filled circles, open and filled squares, and filled diamond correspond to Figs. 10, 11, 12, 13, and 14, respectively.

mode above its otherwise negligible value so that the spatiotemporal driving-force perturbation associated with the subdominant wave can be large enough to periodically pull the dominant mode. Second, the amplitude of the entrained subdominant mode varies with chopping frequency according to the usual response curve. Along the response curve, the oscillation amplitude of the system response is maximum in the center of the entrainment range and falls off to a minimum at the boundaries.

## VI. THE DYNAMICS PHASE DIAGRAM

The dynamical behavior of a driven system can be conveniently analyzed using the dynamics phase diagram for periodically forced oscillations, an experimentally relevant version of which is shown in Fig. 9. Such a diagram can denote quasiperiodic, entrained, and chaotic regions in the parameter space of driving amplitude versus driving frequency. One can embellish the usual diagram with contours of constant  $\alpha$  to discriminate the various degrees of periodic pulling and entrainment [20], where the parameter  $\alpha \equiv M(\tilde{f} - 1)$ ,  $M$  is one-half the ratio of the driving-force amplitude to the undriven-mode amplitude and  $\tilde{f}$  is the ratio of the undriven-mode frequency to the driving-force frequency. The layout of these boundaries and contours depends on the undriven values of the mode's amplitude and frequency. Usually, the specific nonlinearities of a system translate into only quantitative adjustments to the shape of the contours. The most straightforward system to interpret such a diagram is one with a single possible oscillatory mode, i.e., one stable limit cycle. In this case, only changes in driving amplitude and frequency, which are easily represented on the diagram, affect the dynamical behavior. For a multimode oscillator, using units of normalized driving amplitude  $M$  for the driving-amplitude axis clarifies the representation of certain driven-oscillator phenomena.

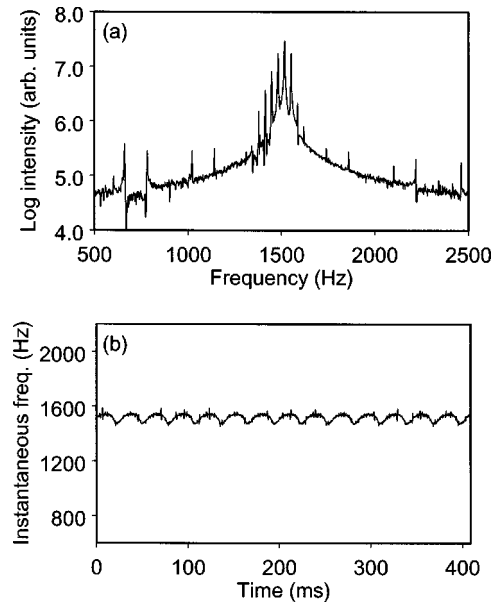


FIG. 10. Signatures of temporal laser-wave interaction ( $f_D = 1519$  Hz). Here the discharge current is 7.51 mA. (a) Spectra and (b) instantaneous frequency.

Temporal periodic pulling, here associated with incomplete laser-wave entrainment ( $\alpha < 1$ ), corresponds to a smaller driving amplitude than its spatiotemporal counterpart, here associated with incomplete wave-wave entrainment ( $\alpha < 1$ ). The latter case involves laser-wave entrainment ( $\alpha \geq 1$ ) as outlined in the middle of the previous section. Figure 9 depicts a simplified dynamics phase diagram that is useful in conceptualizing the differences between the temporal and spatiotemporal cases. Although the values along the frequency axis can be used to conveniently identify a specific case of driving frequency, only the basic features of the entrainment regions are depicted. The case of temporal periodic pulling is indicated by the open triangle, at small driving amplitude, and the case of spatiotemporal periodic pulling is indicated by the filled inverted triangle, at large driving amplitude in Fig. 9. Experimental realizations corresponding to the open triangle and filled inverted triangle are presented in Figs. 10 and 11, respectively.

Figure 10 shows the chopped, neon-resonant light temporally pulling the 1.5 kHz mode. Figure 11 shows the 1.75 kHz mode spatiotemporally pulling the 1.5 kHz mode. The asymmetric spectrum and synchronized modulation of the amplitude and frequency, all inherent in periodic pulling, are obvious in both figures. The amplitude of the frequency modulation is also an important characteristic, to be discussed later. The small (large) separation between spectral features in Figs. 10(a) and 11(a) is related to the narrow (wide) entrainment range associated with such a small (large) driving-force amplitude. The long (short) period in the frequency and amplitude modulation in Figs. 10(b) and 10(c) and 11(b) and 11(c) is related to the pulling-interruption periodicity which is determined by the long (short) time required for the system response to become sufficiently out of phase with the driving force, which, in turn, is related to the frequency difference between them.

Stabilizing the otherwise transient wave-wave periodic pulling process with the laser perturbation requires that one

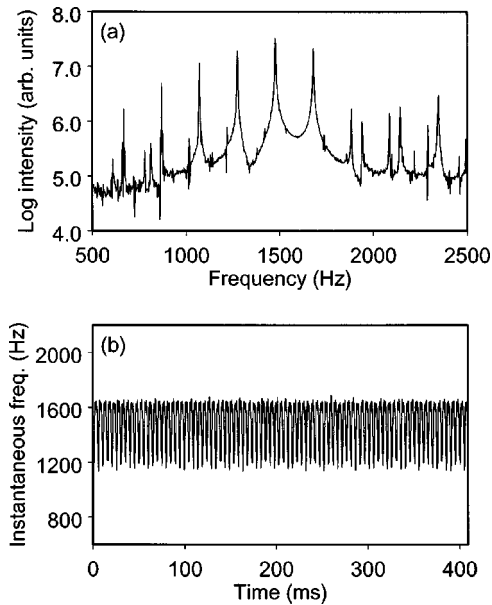


FIG. 11. Signatures of spatiotemporal wave-wave interaction ( $f_D = 1681$  Hz). Here the discharge current is 7.51 mA. (a) Spectra and (b) instantaneous frequency.

of the modes is entrained by the laser. Naturally, leaving the entrainment region will have consequences on this process. As discussed, the boundary can be crossed by changing (1) the driving-force frequency, for example by changing the chopping frequency, (2) the mode's undriven frequency, for example by changing the plasma conditions that influence the spontaneous mode's frequency (e.g., the discharge current), or (3) the effective driving-force amplitude, for example by changing the laser intensity, the laser frequency, or the distance between the laser beam and the cathode.

It is also possible to cross the entrainment boundary by changing the amplitude of the mode being driven. An increase (decrease) in the value of  $M$  can result in a transition into (out of) entrainment. A difference between periodic pulling a dominant mode and a subdominant mode is that the former is associated with a much larger undriven-mode amplitude, and consequently a smaller value of  $M$ . Therefore, a transition that changes a driven oscillatory mode from subdominant to dominant can suddenly decrease the effective driving-force amplitude even if the actual perturbation driving the mode experiences no change at all.

When interpreting the dynamical behavior of a driven multimode oscillator, the driving-amplitude axis of the dynamics phase diagram can be normalized to the mode amplitude, i.e., so that it is labeled in terms of  $M$  as an alternative to considering entrainment-range boundaries that are mode-amplitude dependent. In this way, each combination of driving and mode amplitudes has associated with it an effective value of  $M$  that corresponds to a point on an invariant pattern of entrainment boundaries. In this context, an increase in a driven mode's amplitude is translated into a decrease in the normalized driving-force amplitude at the driving frequency.

## VII. DYNAMICS MODULATION

Under the proper conditions, an incomplete mode transition can take place that is accompanied by an incomplete

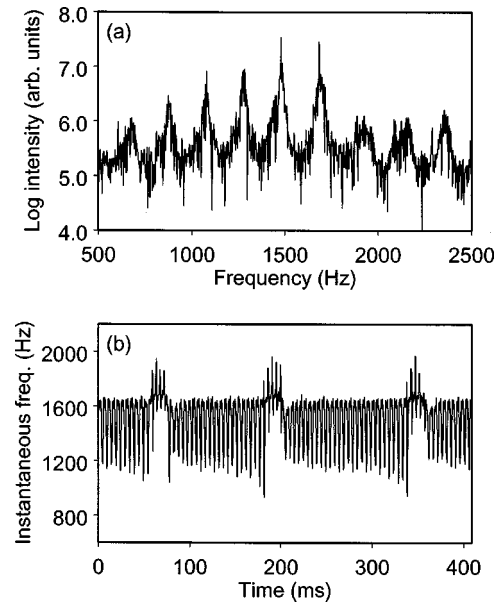


FIG. 12. Signatures of spatiotemporal wave-wave interaction ( $f_D = 1684$  Hz) with periodic mode transitions to the next-higher mode. Here the discharge current is 7.51 mA. (a) Spectra and (b) instantaneous frequency.

transition between temporal and spatiotemporal dynamics. The word incomplete is used to describe a transition that once it occurs, reverses, and then repeats periodically. In a sense, this incomplete transition in the dynamics could be called periodic dynamics pulling, just as periodic frequency (or wavelength) pulling refers to an incomplete transition to entrainment. However, the more general term dynamics modulation, analogous to amplitude and frequency modulation, is more appropriate because the dynamical states flip flop, corresponding to square-wave modulation, whereas pulling implies relaxation-oscillator behavior, more like a saw-tooth modulation. The label bistability is inadequate for describing this phenomenon.

In Figs. 10 and 11, we presented the primary signatures of temporal periodic pulling and of spatiotemporal periodic pulling, respectively. Aspects of both cases are combined in the signatures of dynamics modulation. To demonstrate the dynamics modulation accompanying the incomplete transition between the 1.5 and 1.75 kHz modes, we present Figs. 12 and 13, which illustrate cases wherein the wave-wave pulling of the 1.5 kHz mode by the chopped-light-driven 1.75 kHz mode, with one time scale, is periodically interrupted by a mode transition from 1.5 to 1.75 kHz, with a second time scale, and the reverse transition back to 1.5 kHz, on a third time scale. The laser's influence makes corresponding transitions between temporal entrainment and temporal pulling of the 1.75 kHz mode. The time scales associated with the wave-wave interaction and with the modulation between the wave-wave and laser-wave interactions correspond to distinct features in the plot of the instantaneous frequency and in the spectrum.

In Fig. 12 the degree of periodic pulling is large enough that the upper limit, as well as the overall amplitude, of the frequency modulation inherent in the process increases slightly with time. After 105 ms into each beat period, the instantaneous frequency of the lower mode (i.e., the 1.5 kHz

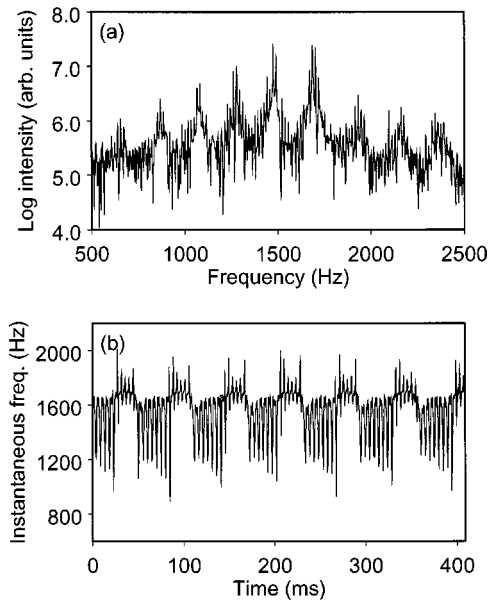


FIG. 13. Signatures of spatiotemporal wave-wave interaction ( $f_D = 1688$  Hz) with more-frequent, periodic mode transitions to the next-higher mode. Here the discharge current is 7.51 mA. (a) Spectra and (b) instantaneous frequency.

mode) becomes close enough to the frequency of the upper mode (i.e., the 1.75 kHz mode) to trigger an upward mode transition, whereupon the 1.75 kHz mode significantly increases its amplitude. The switch in the identity of the dominant mode is apparent in Fig. 12 by the new frequency about which the frequency modulation takes place. Wave-wave periodic pulling is evident even after the mode transition since it takes a fraction of a second for the mode that was formerly dominant to die out [8].

Upon this upward mode transition,  $M$  suddenly decreases and the interaction strength associated with the laser and the 1.75 kHz mode that it is driving decreases sufficiently to interrupt the chopped light's ability to entrain the 1.75 kHz mode. The 1.75 kHz mode immediately assumes its natural frequency. However, with no entrainment, the 1.75 kHz mode is not a very stable limit cycle. Although the laser cannot temporally entrain the dominant mode at 1.75 kHz, the influence of the laser's temporal pulling of the 1.75 kHz mode is strong enough to interrupt the consummation of the upward mode transition before the 1.5 kHz mode decays completely. At this interruption, the system jumps back down in frequency, in a reversal of the upward mode transition, and the process repeats itself.

This temporal periodic pulling process referred to in the previous paragraph is slightly different than the usual case since the relative phase difference between driving force and mode evolves in reverse, i.e., it begins the evolution near the out-of-phase point and ends the evolution near the in-phase point, according to the following explanation. Phase modulation is inherent in the periodic pulling process and during the wave-wave pulling, the two waves begin each beat period in phase with each other and proceed to become more out of phase. The upward mode transition takes place when the 1.75 kHz mode, and the chopped light to which it is synchronized, is sufficiently out of phase with the 1.5 kHz mode. This means the chopped light is initially out of phase

with the newly dominant 1.75 kHz. As the temporal periodic pulling evolves, the phase modulation serves to put back into phase the chopped light and the 1.75 kHz mode. When the chopped light and the 1.75 kHz mode are sufficiently in phase, at which point the laser couples better to the 1.75 kHz mode, the reverse mode transition is induced. This ends the beat period and the system begins the next beat period exactly where it began the previous one, i.e., with the 1.5 and 1.75 kHz modes in phase and involved in spatiotemporal periodic pulling.

In Fig. 13, the spatiotemporal periodic pulling between the dominant 1.5 kHz mode and the subdominant 1.75 kHz mode is stronger than in Fig. 12 due to the increase of the 1.75 kHz mode's amplitude as the chopping frequency becomes closer to the natural mode frequency, according to the usual response curve. The larger driving amplitude and the more rapid increase in the upper limit of the frequency modulation trigger the mode transition slightly earlier in the beat period. The reverse mode transition, on the other hand, requires slightly more time to trigger because, due to the smaller frequency difference between the chopped light and the 1.75 kHz mode it pulls, the phase modulation is slower and therefore it takes longer to put back into phase the chopped light and the 1.75 kHz mode.

Recall from the discussion at the beginning and end of Sec. V that the driving-frequency dependence of the subdominant mode's amplitude is sensitive enough so that as the chopping frequency shifts the subdominant mode toward a neighbor mode's frequency (and away from the subdominant mode's undriven frequency), it can result in a decrease in the degree of periodic pulling. Ordinarily, such a decrease in the frequency difference between the driving force and the system response corresponds to an increase in the degree of periodic pulling, but in the case of the driving force being an entrained mode, the driving amplitude can decrease beyond the amount to compensate for the increase. This counterintuitive effect is most apparent near the limits of the laser-wave entrainment range where the change in  $M$  is largest and the change in  $(\bar{f}-1)$  is smallest.

A comparison between the beat periods shown in Figs. 12(b) and 13(b) reveals that the period of the spatiotemporal segment of the beat period is more sensitive to the period of the temporal segment of the beat period than the adjustment of the chopping frequency. This results in the decrease in the overall beat period and in the increase in the spacing of the spectral fine structure as the chopping frequency is increased. The influence of the beat period associated with the incomplete mode transition on the spectral fine structure can be easily seen in Figs. 11(a), 12(a), and 13(a) as the chopping frequency is increased. A comparison between the temporal periodic pulling in Figs. 10(b), 12(b), and 13(b) suggests that the amplitudes of phase modulation associated with the temporal beat-period segments in Figs. 12(b) and 13(b) are comparable to the  $180^\circ$  phase modulation known to be associated with the conventional temporal pulling case of Fig. 10.

In Fig. 14 the 1.75 kHz mode amplitude is large enough and the frequency difference between the chopping frequency and the 1.75 kHz mode is small enough that the mode transition takes place even faster and the reversal requires even longer. Most important, however, is the frequency difference between the chopping frequency and the

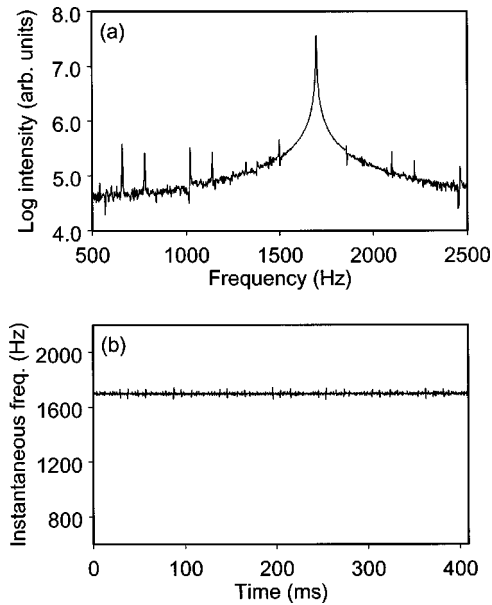


FIG. 14. Signatures of entrainment ( $f_D = 1698$  Hz) at the next-higher mode. Here the discharge current is 7.51 mA. (a) Spectra and (b) instantaneous frequency.

1.75 kHz mode is small enough for the chopping frequency to be within the entrainment region of both the initially subdominant 1.75 kHz mode and the newly dominant 1.75 kHz mode. This results in a complete, as opposed to an incomplete, mode transition and no modulation of the dynamics. Shortly after the application of the driving force, the mode transition takes place, the 1.5 kHz mode completely damps out, and the 1.75 kHz mode stays temporally entrained on the chopping frequency (1.698 kHz) as it was before and throughout the transition. The wave-wave periodic pulling acting before the transition is as transient as that in the undriven cases of Figs. 4–7.

### VIII. DISCUSSION

We can refer to Fig. 9 to understand the interpretation of Figs. 10–14 using the dynamics phase diagram for a multi-mode oscillator. Recall that the normalized vertical scale is in arbitrary units of  $M$ . Each mode has associated with it an entrainment region which has v-shaped boundaries and is identified by the mode's undriven frequency, labeled using a subscript in ascending order based on Fig. 3. The filled triangle, circle, and square are associated with the case of one ionization-wave mode driving, and spatiotemporally pulling, a second mode. The open symbols are associated with the case of chopped light driving, and temporally pulling, the dominant ionization-wave mode. Note that the relative value of  $M$  is large, medium, and small for cases identified with the filled symbols, the open circle and square, and the open triangle, respectively. Figure 10 involves the open triangle case, Fig. 11 involves the filled inverted-triangle case, and Fig. 14 involves the diamond case. Figure 12 (circles) and Fig. 13 (squares) involve periodic transitions between the open and filled symbols.

A discussion of invalid interpretations of Figs. 12 and 13 is warranted. First, we address the possibility that the chopped light entrains the 1.5 kHz mode, and therefore shift-

ing  $f_D$  upward shifts the 1.5 kHz mode closer to the 1.75 kHz mode, first initiating and then enhancing the second periodic pulling process. This cannot be true because the chopping frequency is higher than any of the values of instantaneous frequency associated with the 1.5 kHz mode's frequency modulation, shown in Figs. 10(b), 11(b), 12(b), and 13(b). Thus the possibility is eliminated that the 1.5 kHz mode is entrained by the chopped light. Second, we address the possibility that the temporal entrainment of the 1.75 kHz mode by the chopped light is never interrupted and therefore the incomplete mode transition involves the 1.5 kHz mode periodically jumping to the frequency of the entrained 1.75 kHz mode. This cannot be true because there would be no motivation for the newly dominant 1.75 kHz mode (entrained at 1.698 kHz) to reverse the mode transition since entrainment would stabilize that limit cycle. Third, we address the possibility that the undriven frequency of the higher mode is below 1.698 kHz (perhaps 1.694 kHz, or even 1.68 kHz) instead of above it (i.e., 1.75 kHz), and therefore the newly dominant mode experiences temporal periodic pulling by a driving force with a higher frequency. This cannot be true because there would be no motivation for the reversal of the mode transition, and in the case of the undriven frequency being below 1.681 kHz, there is no way that the degree of spatiotemporal periodic pulling could increase as the frequency difference between the higher and lower modes increases if the driving-force amplitude decreases (according to the response curve associated with the temporal entrainment of the higher mode by the chopped light).

Although some authors have reported quasiperiodic behavior in nonplasma systems, there are no reports of periodic pulling outside the subject of plasma physics. However, there are numerous examples of mode locking in nonplasma systems [21]. Temporal mode locking can occur when a damped pendulum is driven periodically, away from its natural frequency. An example of spatial mode locking is found in charge-density-wave systems, where the spatial periodicity of the charge density wave need not be the same as that of the lattice. A second example occurs in convection of nematic liquid crystals, where the periodicity of the rolls competes with the wavelength of an applied electric field. For the proper conditions, it is expected that these nonplasma systems would exhibit temporal and spatial periodic pulling as well.

Multiple dynamical processes within a single class or in a variety of classes are possible in a single system. For example, absolute and convective instabilities, self-organization, driven-oscillator behavior, and chaos can occur separately in the same system in plasma physics [22], autocatalytic chemical reactions [23], population dynamics [24], etc. Although one dynamical process typically will dominate for a specific set of system conditions, two or more processes may occur simultaneously and, in some cases, can be coupled. For example, the temporal variation of one of the system's control parameters can couple to a temporal or spatiotemporal process. Such coupling has been exploited to increase the yield and selectivity of catalytic [25] and biochemical reactions [26]. In this paper is described the coupling between temporal and spatiotemporal modifications to the metastable population in a neon glow discharge.

In summary, we have investigated the influence of a

chopped and unchopped, single mode laser beam at a metastable transition of  $6401 \text{ \AA}$  ( $1s^5-2p^9$ ) on a neon glow discharge. The degree to which the resonant light influences the discharge is found to depend on the distance of the perturbation from the cathode, as well as the light intensity. The influence of perturbations using other metastable transitions was weaker. The dc light is responsible for mode transitions in the spontaneous oscillations of the neon glow discharge. The chopped light is used to systematically control spatiotemporal perturbations applied to the spontaneous oscillations. The cases of temporal and spatiotemporal periodic pulling are identified by the relative strengths of the interactions. The first observation of dynamics modulation is documented and the phenomenon is described as the modulation between spatiotemporal and temporal processes involving

the crossing and recrossing of the entrainment boundary caused by a mode transition that periodically reverses.

#### ACKNOWLEDGMENTS

Discussions regarding the glow discharge and periodic pulling with Dr. H. Deutsch, Dr. C. Wilke, Dr. A. Piel, and Dr. T. Klinger are gratefully acknowledged. This work was performed under the auspices of DFG Sonderforschungsbereich 198/A8 and the U.S. National Science Foundation. Two authors (K. D. W. and M. E. K.) would like to acknowledge travel support from these agencies and the kind hospitality of the host plasma physics group during the two exchange visits.

- 
- [1] Y. P. Raizer and J. E. Allen, *Gas Discharge Physics* (Springer, Berlin, 1991); X. Wojaczek and A. Rutscher, *Beitr. Plasmaphys.* **3**, 217 (1963); A. Rutscher and K. Wojaczek, *ibid.* **4**, 41 (1964).
- [2] H. Achterberg and J. Michel, *Ann. Phys. (Leipzig)* **2**, 365 (1959); L. Pekárek, *Usp. Fiz. Nauk* **94**, 463 (1968) [*Sov. Phys. Usp.* **11**, 188 (1969)]; L. Pekárek and J. Krása, in *Proceedings of the 7th Yugoslav Symposium and Summer School on the Physics of Ionized Gases*, edited by V. Vujnović (University of Belgrade, Belgrade, 1974), pp. 915–957; R. N. Franklin, *Plasma Phenomena in Gas Discharges* (Clarendon, Oxford, 1976), pp. 166–171.
- [3] L. Pekárek, *Czech. J. Phys., Sect. A* **4**, 221 (1954); K. Wojaczek, *Ann. Phys. (Leipzig)* **2**, 68 (1959).
- [4] K.-D. Weltmann, T. Brauer, H. Deutsch, and C. Wilke, *Contrib. Plasma Phys.* **35**, 225 (1995).
- [5] B. van der Pol, *Proc. IRE* **22**, 1051 (1934).
- [6] C. Hayashi, *Nonlinear Oscillations in Physical Systems* (Princeton University Press, Princeton, NJ, 1985), Parts II, III, and IV, pp. 86–93.
- [7] C. Wilke, H. Deutsch, and R. W. Leven, *Contrib. Plasma Phys.* **30**, 659 (1990).
- [8] M. E. Koepke, T. Klinger, F. Seddighi, and A. Piel, *Phys. Plasmas* **3**, 4421 (1996).
- [9] H. Lashinsky, in *Symposium on Turbulence of Fluids and Plasmas*, Polytechnic Institute of Brooklyn, edited by J. Fox (Polytechnic Press, New York, 1968), pp. 29–46.
- [10] R. H. Abrams, Jr., E. J. Yadlowsky, and H. Lashinsky, *Phys. Rev. Lett.* **22**, 275 (1969).
- [11] M. E. Koepke and D. M. Hartley, *Phys. Rev. A* **44**, 6877 (1991); M. E. Koepke, in *Physics of Space Plasma (1991)*, edited by T. Chang, G. B. Crew, and J. R. Jasperse (Scientific, Cambridge, MA, 1992), p. 393.
- [12] M. E. Koepke, K.-D. Weltmann, and C. A. Selcher, *Bull. Am. Phys. Soc.* **40**, 1716 (1995).
- [13] B. Albrecht, H. Deutsch, R. W. Leven, and C. Wilke, *Phys. Scr.* **47**, 196 (1993).
- [14] K.-D. Weltmann, H. Deutsch, H. Unger, and C. Wilke, *Contrib. Plasma Phys.* **33**, 73 (1993).
- [15] C. Wilke, R. W. Leven, and H. Deutsch, *Phys. Lett. A* **136**, 114 (1989).
- [16] K.-D. Weltmann, T. Klinger, and C. Wilke, *Phys. Rev. E* **52**, 2106 (1995).
- [17] T. Klinger, A. Piel, F. Seddighi, and C. Wilke, *Phys. Lett. A* **182**, 312 (1993).
- [18] J. F. Behnke, H. Deutsch, and H. Scheibner, *Beitr. Plasmaphys.* **25**, 41 (1985); **11**, 23 (1991).
- [19] M. E. Koepke, T. Klinger, F. Seddighi, and A. Piel, *Bull. Am. Phys. Soc.* **38**, 1907 (1993).
- [20] T. Klinger, F. Greiner, A. Rohde, A. Piel, and M. E. Koepke, *Phys. Rev. E* **52**, 4316 (1995).
- [21] H. Haucke and R. Ecke, *Physica D* **25**, 307 (1987).
- [22] V. S. Anishchenko, G. V. Melekhin, V. A. Stephanov, and M. V. Chirkin, *Izv. Vyssh. Uchebn. Zaved., Radiofiz.* **29**, 839 (1986); P. Y. Cheung and A. Y. Wong, *Phys. Rev. Lett.* **59**, 551 (1987); F. Braun, J. A. Lisboa, R. E. Francke, and J. A. C. Gallas, *ibid.* **59**, 613 (1987); J. Qin, L. Wang, D. P. Yuan, P. Gao, and B. Z. Zhang, *ibid.* **63**, 163 (1989); G. Strohlein and A. Piel, *Phys. Fluids B* **1**, 1168 (1989); A. Fasoli, F. Skiff, R. Kleiber, M. Q. Tran, and P. J. Paris, *Phys. Rev. Lett.* **68**, 2925 (1992); J. Chen, *J. Geophys. Res.* **97**, 15011 (1992).
- [23] B. S. Martincigh, M. J. B. Hauser, and R. H. Simoyi, *Phys. Rev. E* **52**, 6146 (1995); B. S. Martincigh and R. H. Simoyi, *ibid.* **52**, 1606 (1995); C. R. Chinake and R. H. Simoyi, *J. Chem. Soc., Faraday Trans.* (to be published).
- [24] *Chaos and Insect Ecology*, edited by J. A. Logan and F. P. Hain (Virginia Agricultural Experiment Station and Virginia Polytechnical Institute and State University, Blacksburg, VA, 1991); J. W. Wilder, N. Voorhis, J. J. Colbert, and A. Sharov, *Ecological Modelling* **72**, 229 (1994); J. W. Wilder, D. A. Vasquez, I. Christie, and J. J. Colbert, *Chaos* **5**, 700 (1995).
- [25] R. Imbihl and G. Ertl, *Chem. Rev.* **95**, 697 (1995).
- [26] R. Y. K. Yang and J. Su, *Bioprocess. Eng.* **9**, 97 (1993).